Computer Standards & Interfaces 63 (2019) 27–42

Contents lists available at ScienceDirect

Computer Standards & Interfaces

journal homepage: www.elsevier.com/locate/csi

A new efficient error control algorithm for wireless sensor networks in smart grid

Melike Yigit*[a], Pinar Sarisaray Boluk[a], V. Cagri Gungor[b]

[a] Department of Computer Engineering, Faculty of Engineering, Bahcesehir University, Ciragan Cad. Osmanpasa Mektebi Sok. No: 4 - 6, Besiktas, Istanbul, 34353, Turkey
[b] Department of Computer Engineering, Faculty of Engineering, Abdullah Gul University (AGU), Barbaros Mahallesi, Erkilet Bulvari, Kocasinan, Kayseri, Turkey

ARTICLE INFO

Keywords:
Error detection and correction
Rs code
Bch code
Smart grid
Multi-channel scheduling
AEC

ABSTRACT

Error detection and correction is an important issue in the design and maintenance of a smart grid communication network to provide reliable communication between sender and receiver. Various error-control coding techniques are employed to reduce bit error rates (BER) in wireless sensor networks (WSNs). The performance of these techniques is also compared and evaluated to find the most suitable technique for WSNs. This is the first study to compare the most efficient coding techniques in the smart grid environment, and it suggests a new error correction algorithm based on this comparison result. Therefore, this article first examines and compares two forward error control (FEC) coding techniques such as Bose-Chaudhuri-Hochquenghem code (BCH) and Reed Solomon code (RS) with various modulation methods including frequency shift keying (FSK), offset quadrature phase-shift keying (OQPSK), and differential phase shift keying (DPSK) in a 500 kV line-of-sight (LoS) substation smart grid environment. Second, as a result of this comparison, a new adaptive error control (AEC) algorithm is proposed. Adaptive error control adaptively changes error correction code (ECC) based on the channel behavior that is observed through the packet error rate (PER) in the recent previous transmissions. The link-quality-aware capacitated minimum hop spanning tree (LQ-CMST) algorithm and the multi-channel scheduling algorithm are used for data transmission over the log-normal channel. Therefore, the performance of compared coding techniques and AEC are also evaluated when multiple channels are used during transmission. Further, AEC is compared with static RS and without-FEC methods based on performance metrics such as the throughput, BER, and delay in different smart grid environments, e.g., 500 kV Substation (LoS), underground network transformer vaults (UTV) (LoS), and main power control room (MPR) (LoS). Our simulation results indicate that the proposed AEC algorithm achieves better performances than all those techniques.

1. Introduction

The smart grid is a modern electric power system that provides power efficiency by integrating novel technologies, including new energy management techniques and metering and sensing technologies into the traditional power grid [1]. Wireless Sensor Networks (WSNs) are the important components of smart grid due to their sensing, monitoring, and networking capabilities that are highly required for smart grid applications [2]. Many parts of the electric power grid, which are generation plants, renewable energy sites etc., use WSNs [3]. Various information types, such as the generation efficiency and the power usage, are measured and transmitted to a sink node [4,5]. WSNs also have other potential application areas, which are physical intruder detection and environment security, in smart grid facilities [6]. However, the performance of WSNs in smart grid applications is affected due to harsh channel conditions of smart grid environments.

The recent WSN platforms can provide reliable and cost-efficient solution for smart grid management systems that monitor and control the real-time performance of the grid [5,7]. In these systems, location tracking and lifetime maximization of sensor nodes can bring several benefits for smart grid applications, including line fault and power theft detection, dynamic thermal rating, outage detection, etc. In this respect, WSNs provide low-cost and power efficient wireless communications for various types of smart grid applications. However, meeting the reliability requirements of smart grid applications depends on reliable communication between all the nodes and the sink node of the sensor network in harsh smart grid environments.

Providing reliable communication links between the electric power utilities and consumers is an important issue of the smart grid. Robust communication can be achieved if the data is transmitted with no error.

* Corresponding author.
E-mail addresses: melike.yigit@stu.bahcesehir.edu.tr (M. Yigit), pinar.sarisaray@eng.bau.edu.tr (P. Sarisaray Boluk), cagri.gungor@agu.edu.tr (V.C. Gungor).

https://doi.org/10.1016/j.csi.2018.11.006
Received 7 May 2018; Received in revised form 22 October 2018; Accepted 14 November 2018
Available online 22 November 2018
0920-5489/

Table 1
WSN-based smart grid applications [16].

Application	Domain
Residential energy management	Consumer Side
Smart metering	Consumer Side
Automated panel management	Consumer Side
Building automation	Consumer Side
Demand-side load management	Consumer Side
Overhead transmission line monitoring	T&D Side
Conductor temperature rating system	T&D Side
Underground cable system monitoring	T&D Side
Outage detection	T&D Side
Real-time generation monitoring	Generation Side
Remote monitoring of wind and solar turbines	Generation Side
Distributed generation	Generation Side

However, achieving error-free transmission in wireless sensor network (WSN)-based smart grid communication systems is difficult since communication channels suffer from many factors such as noise, path loss, fading, shadowing, reflection, and diffraction [8]. Therefore, using a proper error control technique is the most crucial issue to minimize the bit error rate (BER) with a lower delay in the smart grid applications that are presented in Table 1 based on their domains, such as generation side, transmission and distribution (T&D) side, and consumer side. Interrelationships between these components are shown in Fig. 1. Fig. 1 also illustrates an example scenario of Advanced Metering Infrastructure (AMI) application. As shown in this figure, smart meters are installed at users' homes to measure the users' electricity loads in an automated manner via two-way communications between the power utility and users. Smart meters measure and adjust the electricity usage of the users to reduce the energy usage at peak time periods and in this way, providing low electricity bill [3]. To achieve this, consumers and utilities must interact with each other by exchanging the electricity usage and price information. Therefore, the mechanism of AMI application involves the interaction between generation, transmission, and distribution, and the consumer sides by bidirectional transmissions of information and power.

Various error control techniques such as forward error correction (FEC) are used to achieve reliable and secure data transmission over a channel. In these techniques, data are encoded using various algorithms before transmission, and then the receiver decodes the encoded data to get the original data. The efficiency of these error control techniques changes according to the communication channel. Therefore, the performances of these techniques differ even under the same channel conditions.

In the literature, performance comparison of error correcting codes for WSNs is widely done by many authors [8–14]. However, performance comparison of error detection and correction codes by combining various modulation techniques for WSN-based smart grid communication networks is not available in the literature. In this respect, we first analyzed the performance of Hamming code, using different modulation schemes, in a 500 kV substation (line-of-sight (LoS)) smart grid environment in [15]. We found that Hamming code with offset quadrature phase-shift keying (OQPSK) modulation demonstrates the best performance. In this paper, performance comparison of other FEC algorithms such as Bose-Chaudhuri-Hochquenghem code (BCH) and Reed-Solomon RS codes (RS), combined with the modulations including differential phase shift keying (DPSK), frequency shift keying (FSK), and OQPSK are analyzed and compared for the first time in a WSN-based smart grid communication network. We utilized these error correction codes (ECCs) and modulation schemes as ECC and modulation schema since these are well-known codes and schemas, and their performance has been evaluated for WSNs [8,9]. Moreover, BCH and RS codes, and DPSK, FSK, and OQPSK modulation schemas, are easy to implement and their source codes are available for other researchers. Our performance evaluations show that they can efficiently improve network performance in terms of throughput and BER.

A new adaptive error control (AEC) protocol for WSN-based smart grid applications is also proposed. We used RS codes with OQPSK modulation for our AEC protocol because, according to our previous performance measurements, RS codes with OQPSK modulation give the best result regarding throughput and BER in a 500kV substation (LoS) smart grid environment. Different RS codes such as RS(39,35), RS (45,35), RS(51,35), RS(57,35), and RS(63,35) were used to change these codes according to channel conditions adaptively. In the first step, AEC assigns the RS codes to the nodes according to the transmission distance between the sender node and its parent, and performs the first transmission according to this assignment. This assignment was done based on a look-up table that consisted of the suitable RS codes for each distance range [17]. This look-up table was constructed for many simulations. In the second step, a switching criterion was defined according to the number of acknowledgments (ACKs) of P previously transmitted packets [18] that were received inside a window. The packet error rate (PER) of these packets was measured and compared with the predefined threshold to determine whether to switch to a weaker or stronger RS code. A suitable RS code was chosen based on second look-up tables that stored the BER levels of RS codes and the appropriate RS codes that could solve these BER levels according to operating smart grid environments, i.e., 500kV Substation (LoS), underground network transformer vaults (UTV) (LoS), and main power control room (MPR) (LoS). These tables were constructed using a heuristic method. The aim of AEC is to maintain the reliability required by the smart grid application, while balancing the tradeoff between network overhead and reliability. Performance of AEC was analyzed and compared with static RS and without-FEC mechanisms. The simulation results show that the proposed solution can decrease delay by transmitting less redundant bits and obtaining higher throughput than the static RS scheme.

Additionally, link-quality-aware capacitated minimum hop spanning tree (LQ-CMST) algorithm as well as the multi-channel scheduling algorithm were used for data transmission [19,20]. Therefore, performance evaluations were also done by varying the number of channels to quantify how multi-channel communication affects the performance of ECCs in 500kV substation (LoS) smart grid environment and AEC in 500 kV outdoor Substation (LoS), UTV (LoS), and MPR (LoS).

Overall, our contributions in this paper can be summarized as

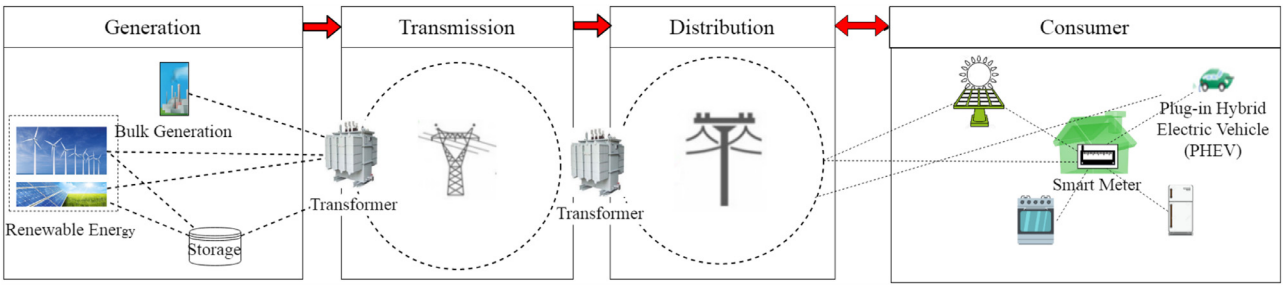

Fig. 1. An overview of Smart Grid network architecture.

follows:

- We performed an in-depth analysis of the performance of RS code, BCH code, and an un-coded channel in terms of throughput, BER, and delay for a WSN-based smart grid application in a 500 kV substation (LoS) smart grid environment. The impact of multi-channel scheduling and type of modulation scheme on the performance of BCH code, RS code, and un-coded channel were presented.
- A new AEC scheme was proposed to meet the reliability requirements of WSN-based smart grid applications according to a switching threshold. The AEC controls the channel conditions and switches to a stronger or weaker code when the PER_{window} is larger than the threshold. The simulation results reveal that our proposed scheme achieves better delay, throughput, and BER results than the static RS coding strategy. In addition, the impact of multi-channel scheduling on the performance of AEC was also evaluated. The results show that multi-channel scheduling improves the performance of AEC in terms of delay, throughput, and BER.
- To the best of our knowledge, there is no study that compares performance of ECCs and proposes a new scheme to detect and correct bit errors for WSN-based smart grid applications. Therefore, studies performed in this paper are the first studies to present the comparative performance evaluations of RS and BCH codes, using different modulation schemes, by applying multi-channel scheduling in a 500kV substation (LoS) smart grid environment. Furthermore, this study is also important since it proposes a new AEC scheme, which can operate in different smart grid environments, i.e., 500 kV outdoor Substation (LoS), UTV (LoS), and MPR (LoS), for WSN-based smart grid applications.

The rest of this paper is organized as follows. An overview of related work on WSN ECC studies is described in Section 2. The proposed AEC algorithm is described in Section 3. The models and assumptions are presented in Section 4. Performance evaluations are discussed in Section 5. Finally, the paper is concluded in Section 6.

2. Related work

In the literature, many studies have compared the error control techniques in WSNs [8–11]. In [8], the performance of RS and BCH codes are compared over a correlated Rayleigh fading channel. The M-quadrate amplitude modulation (M-QAM) is used in the order 16, 32, and 64. Moreover, BER is used as a performance metric in simulations to show the performance of RS and BCH. The results show that the uncoded signal performs better if the modulation order is high. However, if RS and BCH codes are used, BER decreases for all modulation orders. Furthermore, it is also presented that BCH 64-QAM achieves the lowest BER over correlated Rayleigh fading channel. In [9], binary-BCH codes, RS codes, and the convolutional code with Viterbi algorithm are analyzed and compared regarding their power consumption and BER performance on field programmable gate array (FPGA) and application specific integrated circuit (ASIC) platforms. According to the performance comparison of these three error control codes on different platforms, binary-BCH codes perform better than the RS and convolutional codes with Viterbi algorithm if it is used with ASIC implementation. An efficient ECC in terms of BER and power consumption performance is chosen for WSN in [10]. In this respect, BER performance of different ECCs such as RS, Hamming, Golay, and convolutional (Hard) and (Soft) codes are measured and compared. The results show that RS and convolutional codes show better BER performance than the other ECCs. However, RS is more suitable than convolutional codes for WSNs due to the high power consumption of convolutional codes. For this reason, the BER performance of different RS codes is also shown, and RS(31,21) is chosen as the most suitable ECC for WSN. In [11], error control schemes in WSNs are analyzed by using a cross-layer methodology that investigates the cross-layer effects of all layers such as medium access layer, routing layer, and physical layer. Further, FEC, automatic repeat request (ARQ), and hybrid ARQ (HARQ) schemes are analyzed and compared regarding the energy and latency performance. As a result of the cross-layer analysis of error control techniques, the FEC algorithm improves error resiliency since FEC sends redundant bits over the wireless channel. Moreover, it is also shown that end-to-end latency performance of WSNs increases along with targeted PER and energy efficiency when the FEC and the hybrid ARQ schemes are used.

Many studies have been done on adaptive FEC in WSNs [17,18]. In [17], an adaptive FEC coding algorithm at the medium access layer (MAC) is proposed in WSNs. Energy consumption, energy efficiency, PER, recovery overhead, and the quality of the image, defined as the peak-signal-to-noise-ratio (PSNR) value of the image, are the performance metrics of this study in the case of image transmission. This algorithm is based on two look-up tables: namely, a distance look-up table and a BER look-up table. In these look-up tables, the best FEC codes are stored according to different distances and BERs because BER always changes due to changing channel conditions. The proposed algorithm provides a fast solution by selecting the optimum FEC value from the look-up tables. Furthermore, the performance of this algorithm is compared with an adaptive MAC-Level FEC (AMFEC) mechanism [21] and the method of Ghaida et al. [22]. PSNR values of these three methods are compared as the BER of channel changes to evaluate the quality of image transmission. The results show that the proposed algorithm of [17] achieves better performance than the other compared algorithms. This algorithm is effective since it uses look-up tables for quick selection of FEC codes. However, in this algorithm multi-channel scheduling is not considered to be effective for image transmission since it improves the network performance by achieving simultaneous transmission. In [18], an adaptive forward error correction (AFEC) algorithm is proposed for best effort WSNs. A finite state Markov model is used to describe the switching mechanism between the FEC codes. Switching from one state to another in this Markov model is done based on channel conditions that are measured through PER in the last 20 transmissions. If the average PER is higher than the predefined threshold, the current FEC code of the node is changed with a stronger FEC code. The proposed AFEC algorithm is compared with static FEC and an uncoded system. The results reveal that as the switching threshold increases, the throughput performance of AFEC increases as well as PER. This is a consequence of the fact that higher values of the switching threshold imply a less conservative reaction to channel changes, where weaker codes are used most often. The proposed AFEC schema is suitable for best effort WSNs and is not evaluated for smart grid applications. What is more, multi-channel scheduling is also not considered in the proposed schema.

Recently, the methods for error detection and correction have been studied, in order to provide reliable communication in WSNs [23–26]. In [23], a modified relay node selection and corruption aware method is proposed to improve the WSN performance. Different relay selections, such as permanent, reactive, and adaptive, are presented for making efficient relay selection. This relay selection methods are used to increase the error resiliency of a packet via retransmission. However, packets still can be corrupted during transmission. In the proposed method, the receiver detects the corrupted packet and encodes it by using Low Density Parity Check Codes (LDPC). Then the packet is retransmitted. Performance evaluations have been done by using NS2 simulator. Results show that adaptive relay selection gives the best result in terms of latency and energy consumption. The work mentioned in [24] presents a Dynamic and Channel Adaptive Error Control Scheme in Wireless Sensor Networks (DCAECS). DCAECS detects and controls the errors dynamically depending on noise power and channel conditions monitored at the receiver. Channel adaptive and error models are designed to estimate the channel conditions and errors. The proposed DCAECS has channel error estimation, sender, and receiver algorithms. Channel error estimation algorithm estimates the channel condition and measures BER. Depending on the level of BER, sender algorithm

Table 2
RS code according to normalized distance between node and its parent.

Normalized distance between node and its parent	RS Codes
$0 < d \leq 0.22$	RS(39,35)
$0.22 < d \leq 0.34$	RS(45,35)
$0.34 < d \leq 0.44$	RS(51,35)
$0.44 < d \leq 0.55$	RS(57,35)
$0.55 < d \leq 1$	RS(63,35)

chooses the appropriate operating mode. For instance, if the BER level is $10^{-9} \geq BER \geq 10^{-12}$, sender transmits the frame with using simple error control scheme without using retransmission. After the frame is transmitted, receiver receives the frame based on the receiver algorithm. This algorithm firstly controls whether the frame has redundant bits or not. If the frame has redundant bits, it decodes the frame and accept it if there is no error. On the other hand, if the frame does not have the redundant bits, the receiver algorithm check whether the frame lost or damaged. If the frame is not lost or does not have any errors, it accepts the frame, otherwise, the receiver sends negative acknowledgment to the sender. Performance evaluations of DCAECS have been done with simulations. DCAECS have been compared with ARQ Scheme With Adaptive Error Control (ASAEC). Results show that DCAECS performs better than ASAEC in terms of throughput, BER, and probability of retransmission. In [25], an adaptive FEC scheme is proposed for a solar-powered WSN. This scheme is especially designed for a solar-powered WSN because the collected energy in a solar-powered WSN changes severely based on the harvesting environment. For this reason, each node must check energy consumption by considering the energy harvesting rate. The proposed scheme does this control by adaptively adjusting parity length of FEC in compliance with the specified energy budget of a node. RS code is used as the FEC code and an advanced energy-aware RS (EA-RS) scheme is designed. EA-RS consists of three operations that are energy prediction, determination of parity length, and data processing. In energy prediction operation, EA-RS predicts how much energy will be harvested and consumed in the next period. In the determination of parity length operation, EA-RS determines the parity length of the node by considering its energy prediction. In data processing operation, EA-RS collects, encodes, and transmits the encoded data. Performance evaluations have been done to evaluate the performance of EA-RS. RS(36,32), RS(68,32), and the two-level RS scheme are used to compare the EA-RS. Blackout time analysis and received data analysis have been done with simulations. Results show that the proposed EA-RS increases the reliability for WSNs without negatively affecting the blackout time. In [26], a structure, which employs FEC schemes in multi-hop extended star topologies, is proposed. In this proposed structure, extended star topologies are adopted for WSNs and a quantification is done to observe the impact of using FEC scheme via a simulation environment and real-world measurements. Turbo codes are used as a coding scheme. An encoder at the sensor node and an energy-efficient decoder at the base station are implemented. A low-power and low-cost Complex Programmable Logic Device (CPLD) device is applied to mitigate the energy impact on the sensor node. Energy consumption of proposed structure is measured and compared with the ARQ scheme. The results reveal that the proposed scheme is more energy-efficient than the ARQ scheme. Furthermore, simulations on the real platforms also show that although using an advanced FEC scheme increases the cost for sensor nodes, the reductions in number of retransmissions makes it preferable both from low communication delays and energy efficiency.

We observe that all the research studies mentioned above concentrate especially on error detection and correction schemes for WSNs and do not consider the smart grid environments that have harsh channel conditions. Therefore, we firstly analyze the performance of BCH and RS codes with using different modulation schemes, including OQPSK, DPSK, and FSK, in 500kV substation (LoS) smart grid environment and then propose an adaptive error control scheme based on the changing channel conditions with respect to bit error rate. Our proposed approach is compared with static RS and without-FEC schemes in different smart grid spectrum environments, e.g., 500 kV outdoor Substation (Subs), main power control room (MPR), and underground network transformer vaults (UTV).

3. Adaptive error control algorithm

In this section, we describe our proposed AEC algorithm that uses different RS codes with OQPSK modulation. We prefer to use RS codes with modulation since they give the best results according to the simulation results presented in Section 5.1. Here, AEC consists of three steps:

1. Initializing the RS codes of nodes;
2. Creating a look-up table using a heuristic model;
3. Switching between the RS codes based on the threshold.

3.1. Initializing the RS codes of nodes

Our proposed AEC algorithm used different RS codes such as RS (39,35), RS(45,35), RS(51,35), RS(57,35), and RS(63,35). These RS codes were assigned to the nodes according to their distance to their parents. In this respect, we created a look-up table, shown in Table 2, that includes which RS code should be used at which distance. The pseudocode, which was used for creating this look-up table, shown in Algorithm 1. In this algorithm, firstly, we calculated the distances of the nodes to their parents. Secondly, we normalized the distances because nodes were deployed randomly to a $200 \times 200\,m^2$ area and the distances of the nodes to their parents always changed. To handle this change, we had to normalize the distances between the nodes and their parents. As the normalized distance increased, the RS codes with higher code word values (also with more redundant bits) were used. Then, we grouped these normalized values into five categories depending on our RS values (having five different RS values). Finally, we assigned an RS code to each node, depending on their normalized distance. For instance, RS(39,35) was assigned to a node if the normalized distance of the node was between 0 and 0.22, as shown in Table 2.

3.2. Creating a look-up table with using a heuristic model

Providing an optimal solution for specifying which ECC should be used in which BER level was difficult because of the variable channel conditions of WSNs. Therefore, we proposed a heuristic solution that was based on the greedy scheme to determine which RS code provides better results at which BER level for both smart grid environments, i.e., 50 kV substation (LoS), UTV (LoS), and MPR (LoS). Simulations were run many times for each RS code in different smart grid environments, and the BER ranges of these RS codes were found as shown in Tables 3, 4, and 5. Different look-up tables were obtained according to different smart grid environments because BER ranges of these environments and RS codes, which can solve these BER ranges, are varied due to variable channel parameters of smart grid environments as shown in Table 6. Based on the calculated BER, we determined the efficient RS code to find out which RS code could send the packet successfully for each smart grid environment. As a result of this mechanism, we found which BER range could be corrected in which RS code. For instance, we obtained $10^{-4} \leq BER < 10^{-2}$ BER range when we used RS(39,35) with eight channels; and we saw that RS(57,35) could solve this BER range as shown in Table 3. Further, RS(63,35) could also solve this BER range, but we used RS (57,35) to reduce the overhead by sending fewer redundant bits.

Input: parentArray pA;nodeList nL; groupSize grpSize
Output: assignedInitialFECValues

for $n \leftarrow 1$ to nL **do**
    myParent ← pA(node);
    distanceArray(node,myParent) ← calculateEuclideanDistance(node,myParent);
end for

— Normalized Distance —

minDistance ← min(distanceArray);
maxDistance ← max(distanceArray);
biggestDiffDistance ← maxDistance - minDistance;

for $nodeIndex \leftarrow 1$ to $size(distanceArray)$ **do**
    currentNodeDistance ← distanceArray(nodeIndex);
    normalizedDistance ← (currentNodeDistance - minDistance) / (biggestDiffDitance);
    normalizedDistanceArray(nodeIndex) ← normalizedDistance;
end for

— Sort Normalized Distance —

sortedNormalizedDistanceArray ← sort(normalizedDistanceArray);

— Group Normalized Distance —

startIndex ← 0;
sliceSize ←(sortedNormalizedDistanceArray / grpSize);
remainSize ← mod(sortedNormalizedDistanceArray, grpSize);
endIndex ← 0;

for $groupIndex \leftarrow 1$ *to* $grpSize$ **do**
    if $remainSize \neq 0$ **then**
        $endIndex \leftarrow startIndex + 1 + sliceSize$;
        $ditanceGroups(groupIndex) \leftarrow sortedNormalizedDistanceArray(startIndex, endIndex)$;
        $remainSize \leftarrow remainSize - 1$;
    else
        $endIndex \leftarrow startIndex + slizeSize$;
        $distanceGroups(groupIndex) \leftarrow sortedNormalizedDistanceArray(startIndex, endIndex)$;
    end if
    $startIndex \leftarrow endIndex$;
end for

FecArray(grpSize) ← 1, . . . , grpSize;

— Assign Initial FEC Values —

for $groupIndex \leftarrow 1$ *to* $grpSize$ **do**
    $sortedGroupItemList \leftarrow distanceGroups(gorupIndex)$;
    $currentFecValue \leftarrow FecArray(groupIndex)$;
    for $sortedItemIndex \leftarrow 1$ *to* $sortedGroupItemListlength$ **do**
        $itemValue \leftarrow sortedGroupItemList(sortedItemIndex)$;
        $foundIndex \leftarrow findindexofitemValueinnormalizedDistanceArray$;
        if $assignedInitialFecValues(foundIndex) isempty$ **then**
            $assignedInitialFecValues(foundIndex) \leftarrow currentFecValue$;
        end if
    end for
end for

Algorithm 1. Assigning RS codes according to distance.

Table 3
BER levels of RS codes and the appropriate RS codes that can solve these BER levels in 500kV substation (LoS) smart grid environment.

RS Codes	Number of Channel	BER_{min} and BER_{max}	Optimal RS Code
RS(39,35)	1	$10^{-3} \leq BER \leq 1$	RS(63,35)
	8	$10^{-4} \leq BER < 10^{-2}$	RS(57,35)
		$10^{-2} \leq BER \leq 1$	RS(63,35)
	16	$10^{-6} \leq BER < 10^{-4}$	RS(51,35)
		$10^{-4} \leq BER \leq 1$	RS(57,35)
RS(45,35)	1	$10^{-7} \leq BER < 10^{-5}$	RS(51,35)
		$10^{-5} \leq BER \leq 1$	RS(57,35)
	8	$10^{-8} \leq BER < 10^{-6}$	RS(51,35)
		$10^{-6} \leq BER \leq 1$	RS(57,35)
	16	$10^{-9} \leq BER \leq 1$	RS(51,35)
RS(51,35)	1	$10^{-11} \leq BER < 10^{-9}$	RS(57,35)
		$10^{-9} \leq BER \leq 1$	RS(63,35)
	8	$10^{-12} \leq BER < 10^{-9}$	RS(57,35)
		$10^{-9} \leq BER \leq 1$	RS(63,35)
	16	$10^{-14} \leq BER \leq 1$	RS(57,35)
RS(57,35)	1	$0 \leq BER \leq 1$	RS(63,35)
	8	$0 \leq BER \leq 1$	RS(63,35)
	16	$0 \leq BER \leq 1$	RS(63,35)
RS(63,35)	1	$0 \leq BER \leq 1$	RS(63,35)
	8	$0 \leq BER \leq 1$	RS(63,35)
	16	$0 \leq BER \leq 1$	RS(63,35)

Table 4
BER levels of RS codes and the appropriate RS codes that can solve these BER levels in UTV (LoS) smart grid environment.

RS Codes	Number of Channel	BER_{min} and BER_{max}	Optimal RS Code
RS(39,35)	1	$10^{-4} \leq BER \leq 1$	RS(63,35)
	8	$10^{-5} \leq BER \leq 1$	RS(57,35)
	16	$10^{-7} \leq BER < 10^{-5}$	RS(51,35)
		$10^{-5} \leq BER \leq 1$	RS(57,35)
RS(45,35)	1	$10^{-9} \leq BER < 10^{-7}$	RS(51,35)
		$10^{-7} \leq BER \leq 1$	RS(57,35)
	8	$10^{-10} \leq BER \leq 1$	RS(51,35)
	16	$10^{-11} \leq BER \leq 1$	RS(51,35)
RS(51,35)	1	$10^{-12} \leq BER < 10^{-10}$	RS(57,35)
		$10^{-10} \leq BER \leq 1$	RS(63,35)
	8	$10^{-13} \leq BER \leq 1$	RS(57,35)
	16	$10^{-16} \leq BER \leq 1$	RS(57,35)
RS(57,35)	1	$0 \leq BER \leq 1$	RS(63,35)
	8	$0 \leq BER \leq 1$	RS(63,35)
	16	$0 \leq BER \leq 1$	RS(63,35)
RS(63,35)	1	$0 \leq BER \leq 1$	RS(63,35)
	8	$0 \leq BER \leq 1$	RS(63,35)
	16	$0 \leq BER \leq 1$	RS(63,35)

3.3. Switching between the RS codes based on the threshold

Changing RS code in each transmission is not an efficient means in wireless channels since the channel conditions are variable. Therefore, we define a switching mechanism with inspiration from [18]. This mechanism is based on the ACK_s) of S previously transmitted packets received inside a window. The PER inside this window was computed as shown in Eq. (1) by taking the ratio of ACK packets to the S previously transmitted packets.

$$PER_{window} = 1 - \frac{ACK_s}{S} \quad (1)$$

where,

- PER_{window} is the packet error rate within the window,
- ACK_s is the number of acknowledgments that is received within the window,

Table 5
BER levels of RS codes and the appropriate RS codes that can solve these BER levels in MPR (LoS) smart grid environment.

RS Codes	Number of Channel	BER_{min} and BER_{max}	Optimal RS Code
RS(39,35)	1	$10^{-6} \leq BER \leq 1$	RS(57,35)
	8	$10^{-7} \leq BER \leq 1$	RS(51,35)
	16	$10^{-9} \leq BER < 10^{-7}$	RS(51,35)
		$10^{-7} \leq BER \leq 1$	RS(57,35)
RS(45,35)	1	$10^{-10} \leq BER < 10^{-9}$	RS(51,35)
		$10^{-9} \leq BER \leq 1$	RS(57,35)
	8	$10^{-12} \leq BER \leq 1$	RS(51,35)
	16	$10^{-13} \leq BER \leq 1$	RS(51,35)
RS(51,35)	1	$10^{-13} \leq BER < 10^{-11}$	RS(57,35)
		$10^{-11} \leq BER \leq 1$	RS(63,35)
	8	$10^{-14} \leq BER \leq 1$	RS(57,35)
	16	$10^{-18} \leq BER \leq 1$	RS(57,35)
RS(57,35)	1	$0 \leq BER \leq 1$	RS(63,35)
	8	$0 \leq BER \leq 1$	RS(63,35)
	16	$0 \leq BER \leq 1$	RS(63,35)
RS(63,35)	1	$0 \leq BER \leq 1$	RS(63,35)
	8	$0 \leq BER \leq 1$	RS(63,35)
	16	$0 \leq BER \leq 1$	RS(63,35)

Table 6
Log-normal shadowing channel parameters of smart grid environments [29].

Propagation environment	Path loss (γ)	Shadowing deviation (X_σ)
500 kV Substation (LoS)	2.42	3.12
Underground Transformer Vault (LoS)	1.45	2.45
Main Power Room (LoS)	1.64	3.29

- S is the number of previously received packets within the window.

To understand the channel conditions correctly, S should neither be too small nor too large. For higher values of S, using the entire history of packet transmission can cause higher BER since outdated history causes indefinite current channel estimation. On the other hand, smaller values of S prompt frequent changes in the RS code. Therefore, in this study, we chose $S = 15$, as this provided better throughput in 500kV substation (LoS) smart grid environment. Different switching threshold values such as 0, 0.15, and 0.25 were used in AEC in order to analyze how BER, throughput, and delay changed depending on various threshold levels. Pseudocode of our AEC algorithm is shown in Algorithm 2. After initializing the RS code of the nodes, as described in Section 3.1, we assigned new RS values according to this algorithm. In this respect, we first calculated PER_{window}, and if PER_{window} was bigger or equal to our predefined threshold value, we looked at our heuristic tables, shown in Tables 3, 4, and 5 with respect to operating smart grid environment. We iteratively looked at each row of the look-up table and found the current RS code in the table based on the channel. Then, we visited each candidate RS code and controlled the current BER value. If the current BER was between the BER_{MIN} and BER_{MAX} of the candidate RS code, this code was assigned to the node. If there was no BER range that contained the current BER value in our heuristic table, the RS value of the node was not changed. On the other hand, if no error occurred during S transmissions, and if the current RS code was not our first RS code (RS(39,35)), we switched the current RS code to a less powerful RS code (containing less parity bits). Otherwise, if PER_{window} was less than the threshold, we used the same RS value for the next transmission. For instance, assuming that the current RS code of the node was RS(45,35) in channel 1, then the average BER value of S transmissions was 10^{-6}. In this state, AEC assigned the RS(51,35) to the node as a new RS code.

Input: threshold th; perWindow pW; currentRScode rs; allRScodes aRS; heuristicLookupTable h; channel ch; currentBERvalue ber
Output: nextRScode nRS

```
1:  if pW ≥ th then
2:    for i←1 to sizeof h do
3:      heuristicItem ← h(i);
4:      if heuristicItem.channelID == ch AND heuristicItem.RScode == currentRScode then
5:        for i←1 to size of aRS do
6:          possinble nRS ← aRS(i);
7:          if BER_MIN value of possible nRS < ber AND ber ≤ BER_MAX value of possible nRS then
8:            nRS ← possible nRS;
9:          end if
10:       end for
11:     end if
12:   end for
13:   if nRS is not assigned then
14:     nRS ← rs;
15:   end if
16: else
17:   if pW == 0 then
18:     if rs is the first of aRS then
19:       nRS ← rs;
20:     else
21:       nRS ← rs − 1;
22:     end if
23:   else
24:     nRS ← rs;
25:   end if
26: end if
```

Algorithm 2. Assigning RS codes according to threshold and heuristic lookup table.

4. Models and assumptions

4.1. Network model

In this study, we considered a WSN as a graph $G = (V,E)$ in which a set of nodes and a set of edges were shown as V and E, respectively. Cumulative effects of interference in our wireless network were avoided by using a physical interference model. Signal to Interference Noise Ratio (SINR) is used by the physical interference model and nodes receive the packets if the SINR values of the nodes is bigger than a predefined threshold. Information about the SINR calculation can be found in our previous study [19].

We used multi-channel MAC protocol and LQ-CMST routing protocols which were proposed in our previous studies [19,20]. The main motivation behind using these protocols is that they were shown to perform well for WSN-based smart grid applications to improve the network performance by eliminating the impact of bad channel conditions such as interference, noise, and fading.

4.2. General application scenario of AEC

We considered a general WSN-based smart grid application scenario as shown in Fig. 2. It depicts the system using IEEE802.15.4 compliant sensor nodes for both smart grid environments, i.e., 500kV substation (LoS), UTV (LoS), and MPR (LoS). Sensor nodes collect the information and send these information to the sink node. AEC uses different RS codes according to bit error rates. Therefore, these RS codes are also shown in this figure.

This application scenario may be applied on various smart grid applications varying from consumer side applications such as smart metering, building automation, automated panel management, to transmission and distribution side and generation side applications such as outage detection, distributed generation.

Assumptions used for the application scenario of AEC are listed as follows:

- Sensor nodes do not store distance look-up table since this table is used at initial setup and initialization of RS codes is done by the centralized entity.
- Each sensor node stores BER look-up table and uses suitable RS code according to AEC algorithm described in Section 3.
- Energy harvesting scheme [27,28] is integrated with sensor battery system. Hence, the energy consumption is not considered.
- All the sensor nodes except the sink node generate packets.
- Since the physical inference model is used, a node x cannot be scheduled to transmit if the SINR value of its receiver node y is not greater than the SINR threshold value.
- A node does not die while receiving and transmitting the packets during a communication interval.

4.3. Log-normal shadowing model

In this study, log-normal-shadowing model was used to model channels in real channel conditions in different smart grid environments. Log-normal shadowing channel parameters of these smart grid environments are shown in Table 6 [29], i.e. 500 kV Substation, Underground Transformer Vault and Main Power Room. Path loss was computed in the log-normal shadowing model to calculate the link qualities using the following formula:

$$P_L = P_{L_0} + 10\gamma log_{10}(d/d_0) + X_\sigma \quad (2)$$

where,

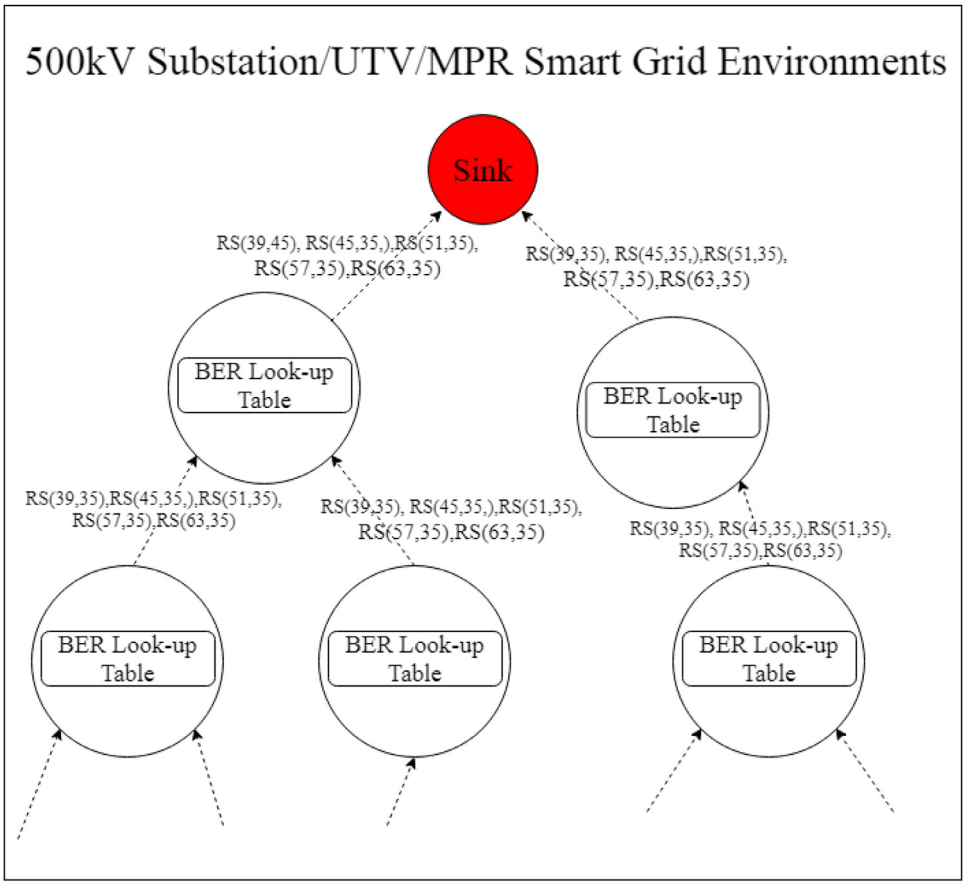

Fig. 2. General application scenario of AEC.

- P_L: path loss with the unit of decibel (dBm),
- P_{L0}: path loss measured in dBm at the reference distance d_0,
- d: path length,
- d_0: reference distance,
- γ: path loss exponent,
- X_σ: Gaussian random variable with standard deviation σ.

4.4. System model

The system model consisted of the following steps: (1) random information symbols k came to the encoder for transmission; (2) the encoder converted each of these information sequences into a unique code word, which consisted of n symbol sequence; (3) the formed code word was sent to a digital modulator; (4) data was transformed into signal waveforms by the modulator using a modulation scheme; (5) the generated signals were sent over the log-normal-shadowing channel for transmission; (6) data could be corrupted during transmission because of the noise in the channel or other factors; (7) a demodulator demodulated the data by separating it from carrier waves; (8) the demodulated data was sent to the decoder, which was located at the receiver side and decoded the data into the original information sequence. The process flow of this system model is shown in Fig. 3.

5. Performance evaluations

In this study, extensive simulations were carried-out using the Matlab environment because the models for multi-channel MAC protocol and LQ-CMST routing protocol were implemented in this environment in previous works [19,20]. The simulation parameters and modulation schemes used in our performance evaluations are shown in Table 7.

5.1. Performance evaluation of RS codes and BCH codes with different modulation schemes

Comparative performance evaluations of the RS and BCH codes and without-FEC algorithm were performed using different modulation schemes in a 500 kV substation (LoS) smart grid environment. Further, BER, throughput, and delay were used as performance metrics in simulations. Fig. 4 compares the BER of without-FEC (uncoded channel) against BCH and RS codes according to different modulation techniques such as DPSK, FSK, and OQPSK. It can be seen from these figures that

Table 7
Simulation parameters and notations .

Parameter	Definition	Values & Notations
Q(.)	Standard Gaussian error function	$Q(x) = \frac{1}{\sqrt{2\pi}} \int_x^\infty exp(-t^2/2)dt$
Eb/No	Signal to noise ratio (SNR)	$Eb/No = \psi \frac{B_N}{R}$
Modulation Schemes	DPSK	$P_b^{DPSK} = \frac{1}{2} exp(-SNR)$
	FSK	$P_b^{FSK} = Q(\sqrt{SNR})$
	OQPSK	$P_b^{OQPSK} = Q(\sqrt{SNR_{DS}})$, $(Eb/No)_{DS} = \frac{(2N \times SNR)}{(N + 4SNR(K-1)/3)}$
P_t	Output Power	4 dB
P_n	Noise Floor	-93dB
#nodes	Number of nodes	120
D_X	Terrain dimension: X	200 m
D_Y	Terrain dimension: Y	200 m
Topology	Topology	Random Topology

BER decreased as the number of channels increased, as multi-channel communication reduced the impact of interference and provided simultaneous transmissions over multiple channels. The results, depicted in Fig. 4(a), show the BER performance of without-FEC, RS, and BCH combined with DPSK modulation. From the graph, it can be observed that RS with DPSK modulation had the best performance with the BER values of 10^{-7}, 10^{-8}, and 10^{-11} obtained for channels 1, 8, and 16, respectively. Fig. 4(b) shows the BER values of without-FEC, RS, and BCH with FSK modulation. It can be seen from the figure that BER values of 10^{-6}, 10^{-7}, and 10^{-9} in RS with FSK modulation is better than BCH and without-FEC. The performance of the without-FEC, RS, and BCH with OQPSK modulation is shown in Fig. 4(c). The results obtained show that the RS with OQPSK modulation had the lowest BER values of 10^{-9}, 10^{-12}, and 10^{-14} at channels 1, 8, and 16, respectively. As a result, it is shown that RS with OQPSK modulation performed best in that it showed the least BER when the number of channels was 16. It also showed that when RS and BCH codes are used, there is a decrease in the BER performance for all modulation schemes.

Figs. 5and 6 compare the delay and throughput of without-FEC (uncoded channel), BCH, and RS codes with different modulation

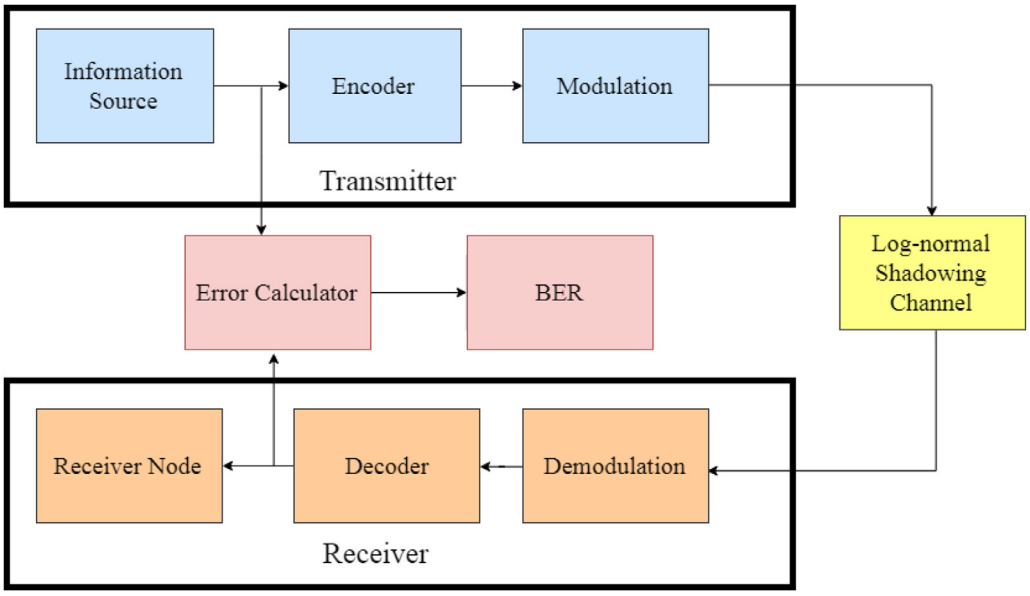

Fig. 3. The process flow of system model.

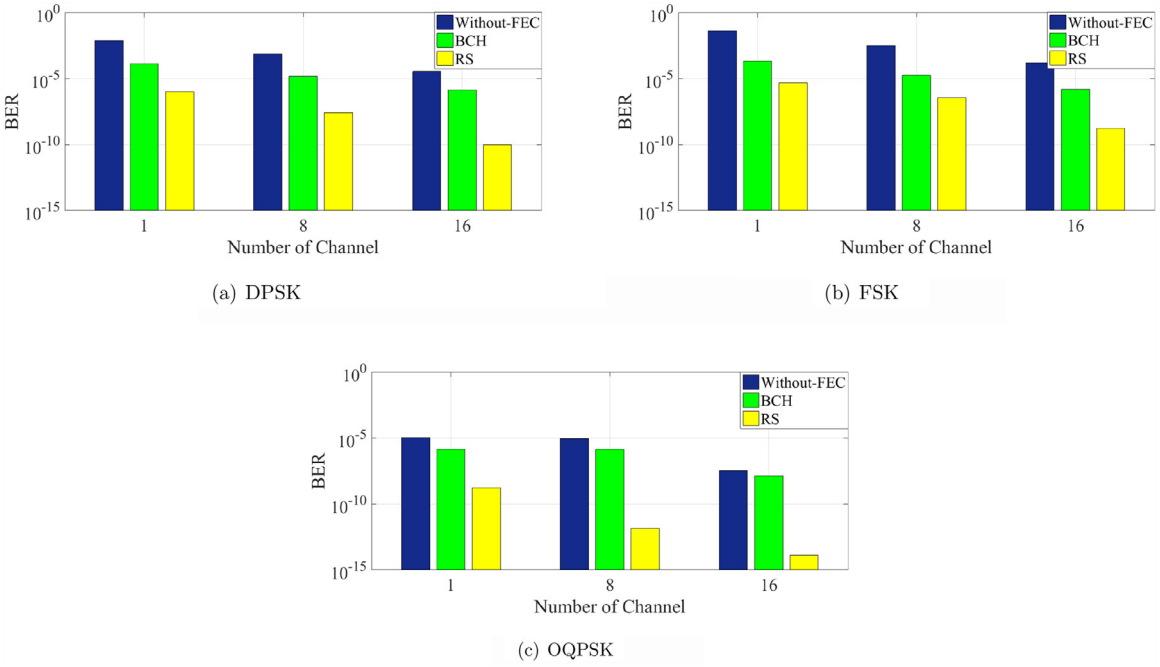

Fig. 4. BER vs. number of channel for log-normal shadowing channel (using DPSK, FSK, and OQPSK) without-FEC, RS, and BCH codes in 500kV substation (LoS) smart grid environment.

techniques in a 500kV substation (LoS) smart grid environment. These results show that delay and throughput performances increase as the number of channels increases for all BCH and RS codes, and un-coded channels because multiple channels avoid interference and provide more simultaneous transmissions to deliver the packets to the sink in a shorter interval. Especially,the throughput results in Fig. 6 show that the performance of BCH and RS codes are better than the un-coded channel, as ECCs detect and correct bit errors, which increases the number of successfully transmitted packets. In addition, Fig. 5 shows that the delay performance of RS and BCH codes is worse than the un-coded channel because RS and BCH codes add redundant bits to the packets to detect and correct the bit errors that cause overheads during transmission and increases transmission delay. In Figs. 5 and 6, it is also observed that the RS with OQPSK modulation is better than the BCH code in terms of throughput and delay.

5.2. *Performance evaluation of AEC algorithm in different smart grid environments*

Extensive simulations were performed to evaluate the performance

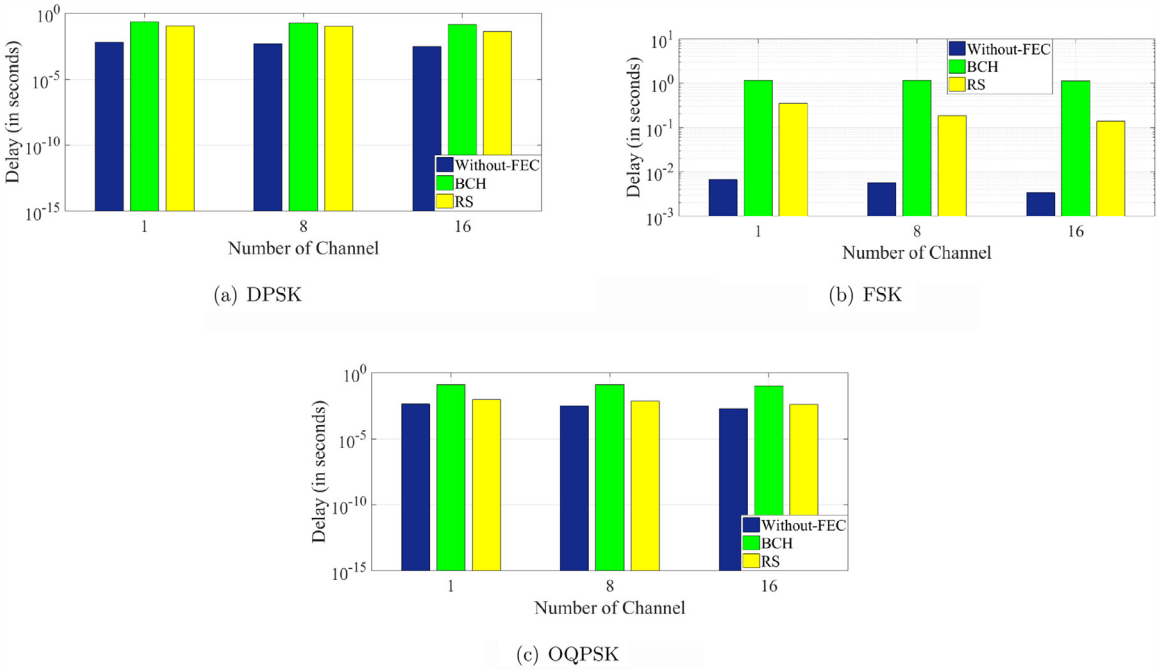

Fig. 5. Delay vs. number of channel for log-normal shadowing channel (using DPSK, FSK, and OQPSK) without-FEC, RS, and BCH codes in 500kV substation (LoS) smart grid environment.

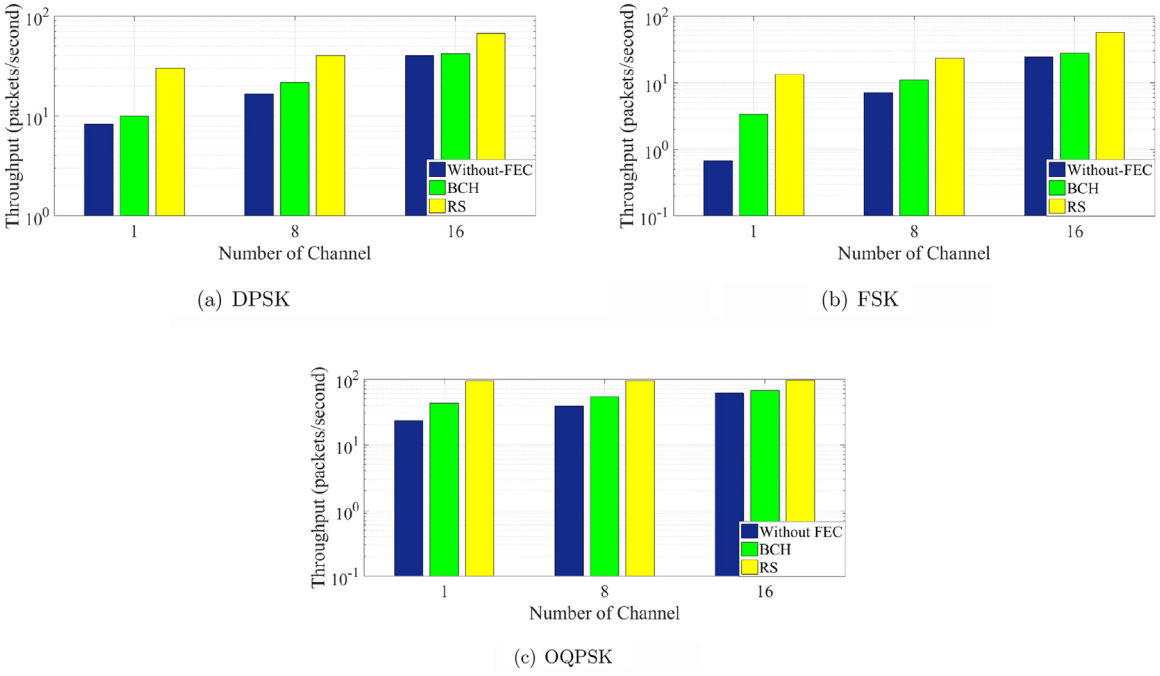

Fig. 6. Throughput vs. number of channel for log-normal shadowing channel (using DPSK, FSK, and OQPSK) without-FEC, RS, and BCH codes in 500kV substation (LoS) smart grid environment.

of AEC in three different smart grid environments, e.g., 500kV substation (LoS), UTV (LoS), and MPR (LoS). These were constituted as follows: AEC uses the transmission history of the nodes to estimate the channel conditions and therefore each node transmitted multiple packets. However, in the simulation model used for RS and BCH codes, whereby each node sent only one packet. Moreover, an OQPSK modulation was used as the modulation scheme since it exhibits better performance than DPSK and FSK modulation schemes. We implemented static RS and without-FEC (un-coded channel) in order to compare them with AEC. The network performance with each AEC, static RS, and without-FEC was evaluated in terms of throughput, BER, and delay. Furthermore, simulations were also performed to show how the multi-channel scheduling affects throughput, BER, and delay of these methods for different threshold values such as 0, 0.15, and 0.25, as in [18] in three different smart grid environments. Accordingly, in the following subsections, simulation results are presented with respect to analysis of BER, delay, and throughput, respectively.

5.2.1. Analysis of BER

In this section, the BER results of the simulations for the different smart grid environments are presented. Figs. 7–9 show the BER performance of the AEC, static RS, and without-FEC in 500 kV substation (LoS), UTV (LoS), and MPR (LoS) smart grid environments, respectively. We see that the BER of AEC is lower than that of static RS and without-FEC for all the threshold values in all smart grid environments. We also observe that as the threshold increases from 0 to 0.25, the BER of the AEC also increases for the both smart grid environments. The reason for this is that when the threshold is 0.25, the number of erroneous packets increased since the new RS code is not assigned until the PER_{window} is not equal to or larger than 0.25. Furthermore, we also notice that, as the number of channels increases, the BER performance of all schemes increases. In Figs. 7–9, it is observed that the best BER result is obtained when using AEC at threshold 0 and channel 16 because AEC immediately changes the RS code, according to the operating environments' look-up tables shown in Tables 3, 4, 5, when the bit error occurs. For instance, if the operating smart grid environment is 500kV substation (LoS), AEC uses the Table 3 to determine new RS code according to the BER result.

In Figs. 7–9, it is observed that BER results obtained in MPR (LoS) environment is better than the BER results measured in 500kV substation (LoS) and UTV (LoS) environments. The reason behind this is that the MPR environment has better channel quality than the other smart grid environments in terms of path loss and shadowing deviation parameters. Therefore, link qualities of MPR environment is better and less affected by interference that occurs due to simultaneous transmissions.

5.2.2. Analysis of delay

Figs. 10–12 show delay results of without-FEC, static RS, and AEC for three different switching thresholds in 500kV substation (LoS), UTV (LoS), and MPR (LoS) smart grid environments, respectively. We have obtained the similar results for both smart grid environments. According to the results, without-FEC always provides the lowest delay among the schemes since it makes no error correction and detection during transmission that cause extra overhead in all smart grid environments. We also observe that as the number of channels increases from 1 to 16, delay of all schemes decreases as multiple channels provide parallel transmission that reduces packet delivery time. Furthermore, the results show that AEC provides lower delay than the static RS schema for all switching threshold values because AEC changes the RS codes according to channel conditions so as to prevent sending unnecessary redundant bits. In this way, AEC causes lower overhead than the static RS schema. In addition, as the switching threshold value increases from 0 to 0.25, the delay of AEC decreases. This is because higher values of switching thresholds indicates a less conservative reaction to channel conditions, where lower codes that have fewer redundant bits are used often, and less transmission is required to transmit the same amount of data bits compared to the codes that provide higher reliability with lower threshold values. For instance, if the threshold value is 0 and current RS code of the node is RS(39,45) in 500kV substation (LoS) smart grid environment, node will immediately change its RS code from RS(39,35) to RS(63,35) according to the Table 3 when the number of channels is 1 and BER range is between $10^{-3} \leq BER \leq 1$. This causes to use extra redundant information that can be unnecessary due to variable channel conditions in smart grid environment. However, if the 0.25 is used as the threshold value, RS

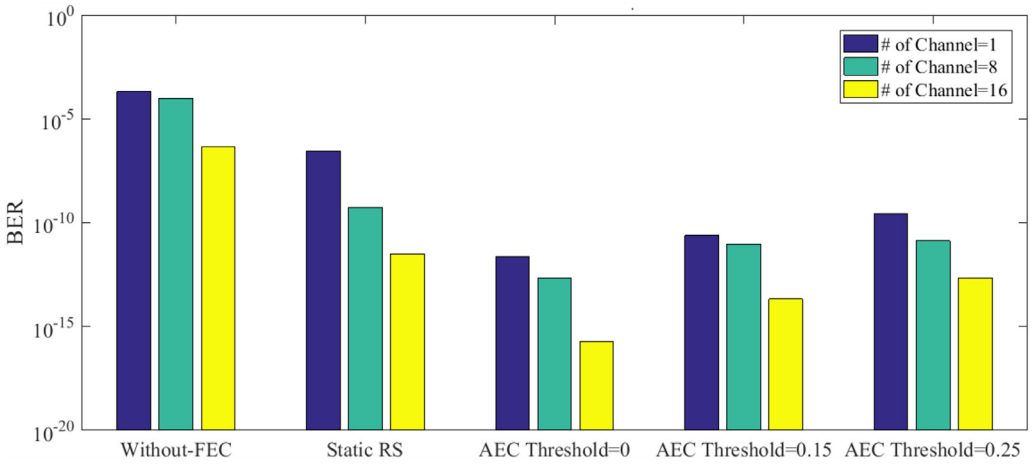

Fig. 7. Comparison of BER of the static RS, without-FEC, and AEC as the number of channels increases at different thresholds of AEC in 500kV substation (LoS) smart grid environment.

code of the node is not changed until the PER_{window} is equal or bigger than the 0.25 and RS(39,35) will continue to be used. In this way, data is transmitted with less redundant bits that provides lower overhead.

In Figs. 10–12, it is observed that delay of algorithms decreases better in MPR (LoS) environment than other evaluated smart grid environments due to better channel characteristics of MPR (LoS) environment. Overall, without-FEC algorithm shows the highest performance in terms of delay in MPR (LoS) environment, since this algorithm does not use make error detection and correction. AEC shows the second best delay result in MPR (LoS) environment when the threshold value is 0.25 because it uses less redundant bits than the static RS at higher threshold values.

5.2.3. Analysis of throughput

Figs. 13–15 show the throughput performance of all performed schemes in different smart grid environments that are 500kV (Los), UTV (LoS), and MPR (LoS), respectively. We obtain the similar throughput results in all smart grid environments. Accordingly, we observe that when the number of channel increases from 1 to 16, throughput performance of all schemes increases for both smart grid environments as multi-channel scheduling overcomes the impact of interference and achieves simultaneous transmission over multiple channels. We also observe that throughput performance of AEC is better than without-FEC and static RS in all environments as it is better than without-FEC because without-FEC makes no error detection and correction algorithm, and therefore, many packets drop during transmission. Static RS also cannot catch the performance of AEC for all switching threshold values and both environments since AEC always changes the RS codes according to channel conditions. Therefore, AEC does not use unnecessary redundant bits that increase the delay of transmission (delay and throughput are inversely proportional to each other). Furthermore, we also investigated the impact of the switching threshold on delay performance of AEC scheme. We observe that as the threshold increases from 0 to 0.25, throughput increases and the highest throughput is obtained when threshold is 0.25 at channel 16 because when the threshold increases, AEC uses the RS codes that provide higher code rates (# of data bits / # of code word bits). For instance, code rate of RS (39,35) is higher than the code rate of RS(45,35). Code rates of our RS codes are shown in Table 8. Moreover, AEC with a 0.25 threshold value uses the weaker codes more frequently than the AEC with 0 threshold and 0.15 threshold as it makes fewer jumps to the stronger codes. Weaker codes have higher code rates and send fewer redundant bits which decrease the delay. For example, if the threshold value is 0 and the current RS code of the node is RS(45,35) in 500kV substation (LoS) environment, node will immediately change its RS code from RS(45,35) to RS(57,35) according to Table 3 when the number of channels = 8 and the BER range is between $10^{-6} \leq BER \leq 1$. RS(57,35) has lower code rate than the RS(45,35) and causes to send extra redundant bits to transmit same amount of data that decreases the throughput. However, if 0.15 or 0.25 is used as the threshold value, the RS code of the node is not changed until the PER_{window} is equal or bigger than the 0.15 or 0.25 and RS(45,35) will continue to be used. This provides to increase network throughput.

In Figs. 13–15, the best throughput results are measured in MPR (LoS) environment, since this environment has better channel quality than other smart grid environments. Furthermore, results also show that AEC with a 0.25 threshold shows the highest performance in terms of network throughput in MPR (LoS) environment.

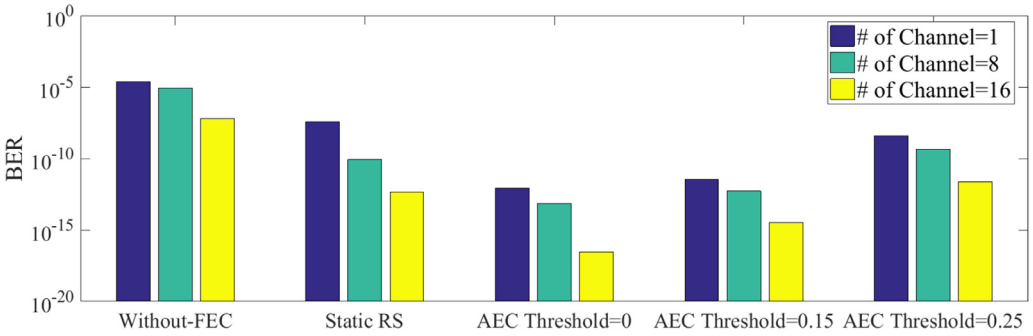

Fig. 8. Comparison of BER of the static RS, without-FEC, and AEC as the number of channels increases at different thresholds of AEC UTV (LoS) smart grid environment.

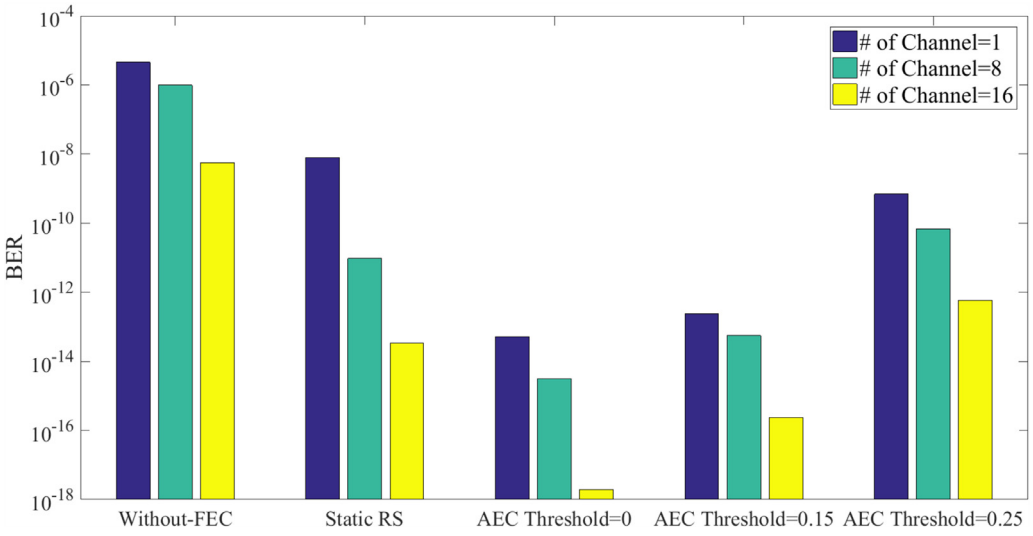

Fig. 9. Comparison of BER of the static RS, without-FEC, and AEC as the number of channels increases at different thresholds of AEC MPR (LoS) smart grid environment.

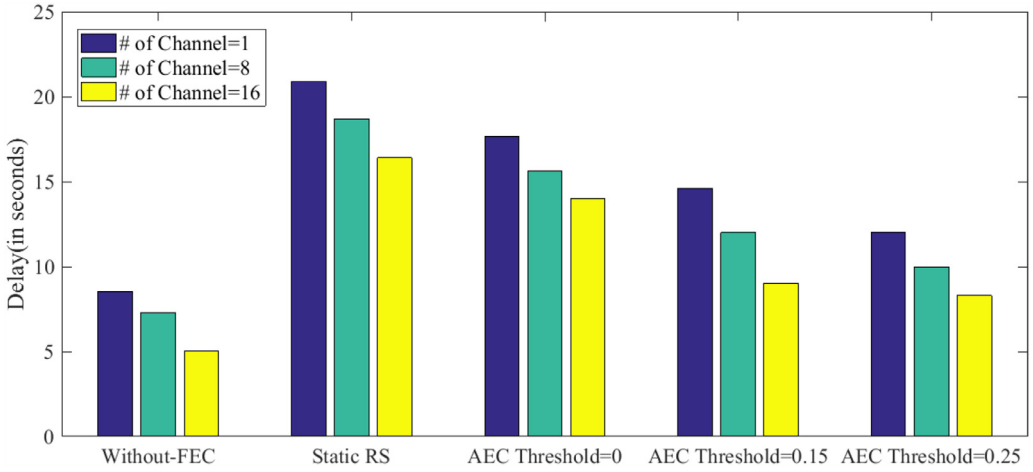

Fig. 10. Comparison of delay of the static RS, without-FEC, and AEC as the number of channels increases at different thresholds of AEC in 500 kV substation (LoS) smart grid environment.

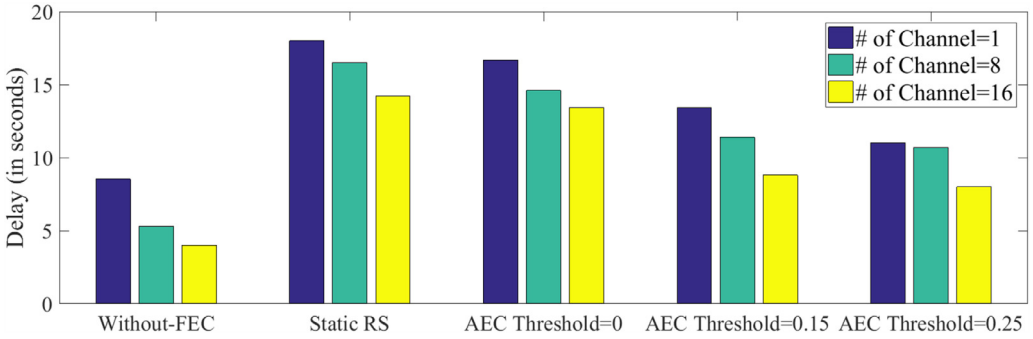

Fig. 11. Comparison of delay of the static RS, without-FEC, and AEC as the number of channels increases at different thresholds of AEC UTV (LoS) smart grid environment.

6. Conclusions and future work

Field tests show that the smart grid has harsh environmental conditions such as noise, interference, and fading. Using an error detection and correction code can solve all of these problems by reducing bit errors during transmission. Selecting an efficient ECC is important for WSN-based smart grid applications. In this respect, in this paper, delay, throughput, and the BER performance of RS code, BCH code, and without-FEC in a 500kV substation (LoS) smart grid environment were first compared using different modulation schemes. Simulations were also performed to evaluate the impact of the number of channels on delay, throughput, and BER. The performance evaluations were done to determine quantitatively how much communication delay, BER, and throughput of the network change when the number of channels

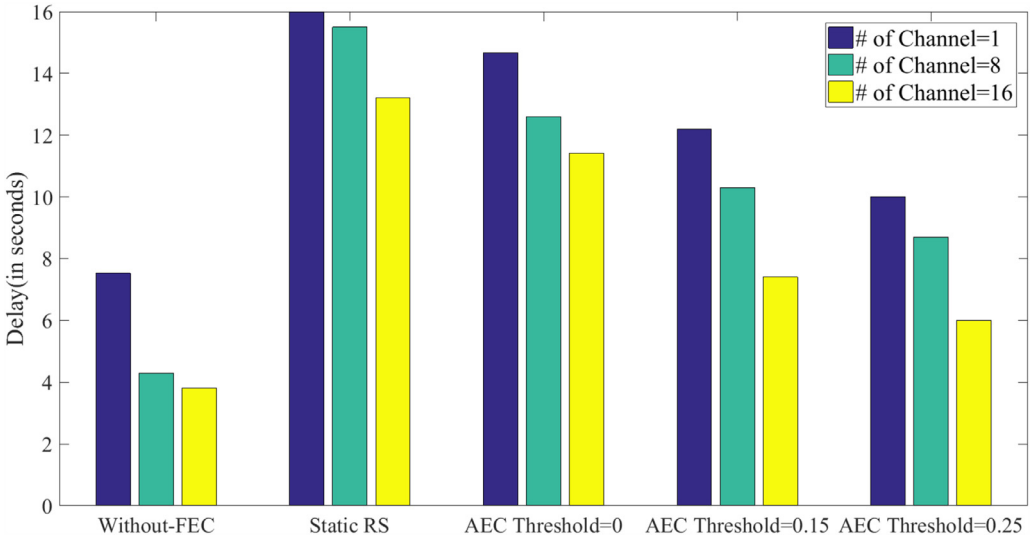

Fig. 12. Comparison of delay of the static RS, without-FEC, and AEC as the number of channels increases at different thresholds of AEC MPR (LoS) smart grid environment.

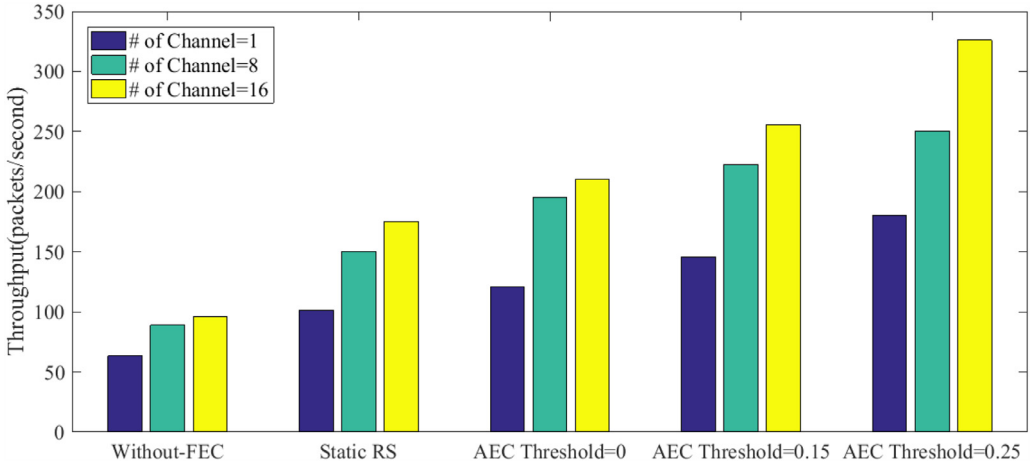

Fig. 13. Comparison of throughput of the static RS, without-FEC, and AEC as number of channels increases at different thresholds of AEC in 500 kV substation (LoS) smart grid environment.

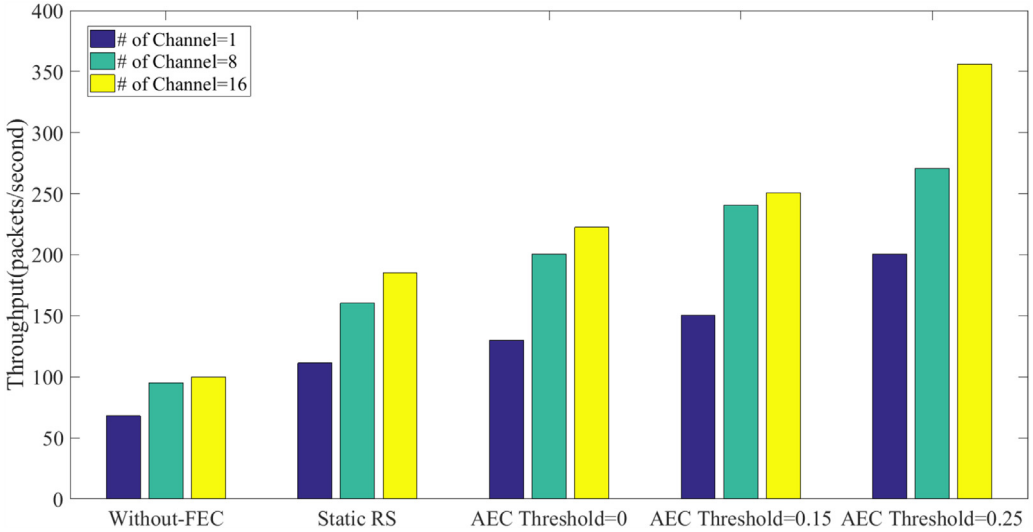

Fig. 14. Comparison of throughput of the static RS, without-FEC, and AEC as number of channels increases at different thresholds of AEC UTV (LoS) smart grid environment.

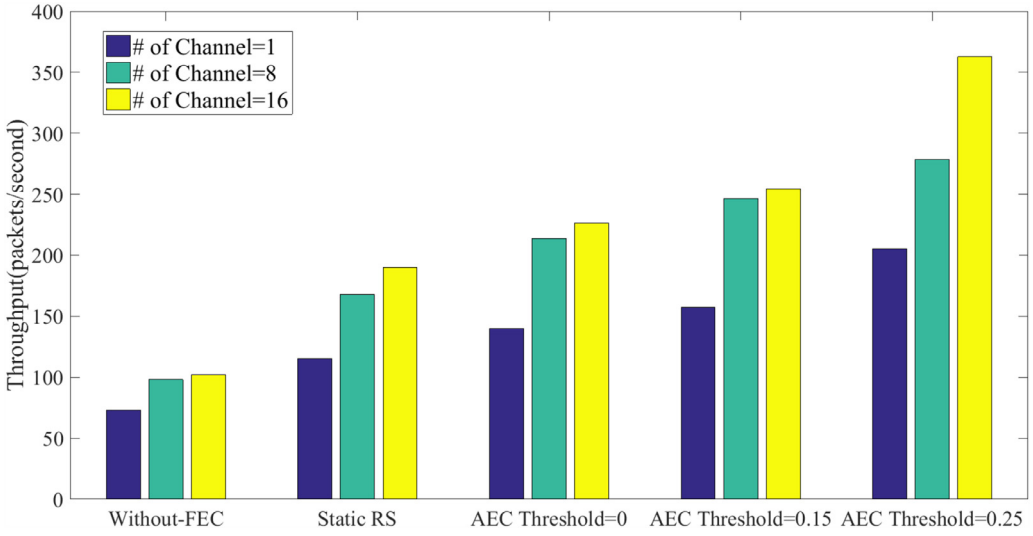

Fig. 15. Comparison of throughput of the static RS, without-FEC, and AEC as number of channels increases at different thresholds of AEC MPR (LoS) smart grid environment.

Table 8
Code rates of RS codes.

RS Codes	Code Rate
RS(39,35)	0.897
RS(45,35)	0.778
RS(51,35)	0.686
RS(57,35)	0.614
RS(63,35)	0.556

increases. Then, a new AEC method was proposed for WSN-based smart grid applications. This scheme firstly assigned the RS codes according to distance between the node and its parent, and then used one of the look-up tables, which are constructed for different smart grid environments, i.e., 500kV substation (Los), UTV (LoS), and MPR (LoS), in order to determine the jump values of RS codes. These look-up tables were constructed in a heuristic way by measuring the BER ranges of each RS code for different numbers of channels in each different smart grid environments. The impact of multi-channels on the BER range of RS codes was also analyzed. Wireless channel conditions in smart grid environments can vary greatly. Therefore, changing the RS code according to the current BER value by using the heuristic look-up table is not suitable for these variable mediums. In this respect, a threshold mechanism was used according to the history of recent transmitted packets using ACKs packets. Different threshold values were used in order to observe how the threshold change affected the performance of our algorithm. Furthermore, the impact of multi-channels on the performance of AEC was also analyzed. The results showed that when multi-channels were used, the performance of all schemes improved for both smart grid environments. Based on the simulations, it was observed that the performance of AEC differs in terms of throughput, BER, and delay in different threshold values. Therefore, before making a decision for network design in different smart grid environments, the requirements of WSN-based smart grid applications must be considered to improve the network performance. If the application requires less BER, AEC can be used with 0 threshold value. However, if the application needs high throughput, AEC should be used with 0.25 threshold value. This study is the first study that proposes a new FEC schema and makes performance comparison with other error detection and correction codes for smart grid applications. In this respect, we expect that this study will motivate the research community to further explore this promising research area.

This study is the first step towards Adaptive Error Control for WSNs in smart grid. The next stage should include bench-marking with polar codes since polar codes provide higher reliability for sensor networks and investigating the energy efficiency of the proposed method. Finally, the real test-bed experiments should be also presented to verify the proposed concept.

Acknowledgement

The work of V.C. Gungor was supported by the BAGEP Award of the Science Academy and AGUV Foundation.

Supplementary material

Supplementary material associated with this article can be found, in the online version, at 10.1016/j.csi.2018.11.006

References

[1] Q. Zeng, H. Li, D. Peng, Frequency-hopping based communication network with multi-level qoss in smart grid: code design and performance analysis, IEEE Trans. Smart Grid 3 (4) (2012) 1841–1852.
[2] S. Kurt, H.U. Yildiz, M. Yigit, B. Tavli, V.C. Gungor, Packet size optimization in wireless sensor networks for smart grid applications, IEEE Trans. Ind. Electron. 64 (3) (2017) 2392–2401.
[3] V.C. Gungor, D. Sahin, T. Kocak, S. Ergut, C. Buccella, C. Cecati, G.P. Hancke, A survey on smart grid potential applications and communication requirements, IEEE Trans. Ind. Inf. 9 (1) (2013) 28–42, https://doi.org/10.1109/TII.2012.2218253.
[4] M. Chen, Reconfiguration of sustainable thermoelectric generation using wireless sensor network, IEEE Trans. Ind. Electron. 61 (6) (2014) 2776–2783.
[5] S.B. Shah, C. Zhe, F. Yin, I.U. Khan, S. Begum, M. Faheem, F.A. Khan, 3D weighted centroid algorithm & rssi ranging model strategy for node localization in wsn based on smart devices, Sustain. Cities. Soc. 39 (2018) 298–308.
[6] M. Li, H.-J. Lin, Design and implementation of smart home control systems based on wireless sensor networks and power line communications, IEEE Trans. Ind. Electron. 62 (7) (2015) 4430–4442.
[7] S.B.H. Shah, C. Zhe, S.H. Ahmed, Y. Fuliang, M. Faheem, S. Begum, Depth based routing protocol using smart clustered sensor nodes in underwater wsn, Proceedings of the 2nd International Conference on Future Networks and Distributed Systems, ACM, 2018, p. 53.
[8] D.O. Akande, F. Ojo, R. Abolade, Performance of rs and bch codes over correlated rayleigh fading channel using qam modulation technique, J. Inf. Eng. Appl. 4 (2014) 88–94.
[9] G. Balakrishnan, M. Yang, Y. Jiang, Y. Kim, Performance analysis of error control codes for wireless sensor networks, Information Technology, 2007. ITNG'07. Fourth International Conference on, IEEE, 2007, pp. 876–879.
[10] M.R. Islam, Error correction codes in wireless sensor network: an energy aware approach, Int. J. Comput. Inf.Eng. 4 (1) (2010) 59–64.
[11] M.C. Vuran, I.F. Akyildiz, Error control in wireless sensor networks: a cross layer analysis, IEEE/ACM Trans. Netw. 17 (4) (2009) 1186–1199.
[12] N.A. Alrajeh, U. Marwat, B. Shams, S.S.H. Shah, Error correcting codes in wireless sensor networks: an energy perspective, Appl. Math. 2 (9) (2015) 809–818.

[13] M.S. Leeson, S. Patel, Energy efficiency of coding schemes for underwater wireless sensor networks, Technological Breakthroughs in Modern Wireless Sensor Applications, IGI Global, 2015, pp. 27–55.
[14] C. Okeke, M. Eng, A comparative study between hamming code and reed-solomon code in byte error detection and correction, Int. J. Res. Appl. Sci. Eng. Technol. (IJRASET) 3 (12) (2015) 34–39.
[15] M. Yigit, V.C. Gungor, P. Boluk, Performance analysis of hamming code for wsn-based smart grid applications, Turkish J. Electr. Eng.Comput. Sci. 26 (1) (2018) 125–137.
[16] V.C. Gungor, D. Sahin, T. Kocak, S. Ergut, C. Buccella, C. Cecati, G.P. Hancke, A survey on smart grid potential applications and communication requirements, IEEE Trans. Ind. Inf. 9 (1) (2013) 28–42.
[17] T.-N. Pham, M.-F. Tsai, T.-Y. Wu, N. Guizani, An algorithm for the selection of effective error correction coding in wireless networks based on a lookup table structure, Int. J. Commun. Syst. 30 (17) (2017).
[18] K. Yu, F. Barac, M. Gidlund, J. Åkerberg, Adaptive forward error correction for best effort wireless sensor networks, Communications (ICC), 2012 IEEE International Conference on, IEEE, 2012, pp. 7104–7109.
[19] M. Yigit, O.D. Incel, V.C. Gungor, On the interdependency between multi-channel scheduling and tree-based routing for wsns in smart grid environments, Comput. Netw. 65 (2014) 1–20.
[20] M. Yigit, V.C. Gungor, E. Fadel, L. Nassef, N. Akkari, I.F. Akyildiz, Channel-aware routing and priority-aware multi-channel scheduling for wsn-based smart grid applications, J. Netw. Comput. Appl. 71 (2016) 50–58.
[21] M.-F. Tsai, N. Chilamkurti, C.-K. Shieh, A. Vinel, Mac-level forward error correction mechanism for minimum error recovery overhead and retransmission, Math. Comput. Model. 53 (11–12) (2011) 2067–2077.
[22] G.A. Al-suhail, K.W. Louis, T.Y. Abdallah, Energy efficiency analysis of adaptive error correction in wireless sensor networks, Int. J. Comput. Sci. Iss. 9 (4) (2012) 79–84.
[23] M. Parameswari, T. Sasilatha, Cross-layer based error control technique for wsn with modified relay node selection and corruption aware method, Wireless Pers. Commun. 99 (1) (2018) 479–495.
[24] R.C.B. Mallanagouda Patil, Dynamic and channel adaptive error control scheme in wireless sensor networks, Global J. Comput. Sci. Technol. (2017).
[25] M. Kang, D. Noh, I. Yoon, Energy-aware control of error correction rate for solar-powered wireless sensor networks, Sensors 18 (8) (2018) 2599.
[26] A. Brokalakis, I. Chondroulis, I. Papaefstathiou, Extending the forward error correction paradigm for multi-hop wireless sensor networks, New Technologies, Mobility and Security (NTMS), 2018 9th IFIP International Conference on, IEEE, 2018, pp. 1–5.
[27] H.U. Yildiz, V.C. Gungor, B. Tavli, A hybrid energy harvesting framework for energy efficiency in wireless sensor networks based smart grid applications, 2018 17th Annual Mediterranean Ad Hoc Networking Workshop (Med-Hoc-Net), IEEE, 2018, pp. 1–6.
[28] J. Han, J. Hu, Y. Yang, Z. Wang, S.X. Wang, J. He, A nonintrusive power supply design for self-powered sensor networks in the smart grid by scavenging energy from ac power line, IEEE Trans. Ind. Electron. 62 (7) (2015) 4398–4407.
[29] V.C. Gungor, B. Lu, G.P. Hancke, Opportunities and challenges of wireless sensor networks in smart grid, IEEE Trans. Ind. Electron. 57 (10) (2010) 3557–3564.

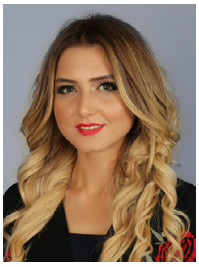

Melike Yigit received her B.S., M.S., and Ph.D. degrees in computer engineering from Bahcesehir University, Istanbul, Turkey, in 2010, 2012, and 2018, respectively. Currently, she works at Turkish Airlines (THY), which is an international airlines in Turkey, as a Business Analyst. Before starting THY, she worked in Huawei Technologies Co. Ltd. and Alcatel-Lucent Teletas as a software developer and San-Tez Project student, respectively. Her current research interests are smart grid communications, power line communications and wireless ad-hoc and sensor networks.

Pinar Sarisaray Boluk received the M.S. and B.S. degrees in Computer Engineering from Karadeniz Technical University, Trabzon. She earned the Ph.D. Degree in the Computer Engineering Department at Istanbul Technical University, Istanbul. She did postdoctoral training at the Computer Science Department of Southern Illinois University in 2013. Currently, she is serving as an Assisted Professor at Software Engineering Department of Bahcesehir University; Istanbul. Her research interests are Wireless Sensor Networks, Network Security, Software Development, Analysis and Design.

Vehbi Cagri Gungor received his B.S. and M.S. degrees in Electrical and Electronics Engineering from METU, Ankara, Turkey, in 2001 and 2003, respectively. He received his Ph.D. degree in electrical and computer engineering from the Broadband and Wireless Networking Laboratory, Georgia Institute of Technology, Atlanta, GA, USA, in 2007. Currently, he is a Professor and Chair of Computer Engineering Department, Abdullah Gul University (AGU), Kayseri, Turkey. His current research interests are in smart grid communications, machine-to-machine communications, next-generation wireless networks, wireless ad hoc and sensor networks, cognitive radio networks, and IP networks. Dr. Gungor has authored several papers in refereed journals and international conference proceedings, and has been serving as an editor, reviewer and program committee member to numerous journals and conferences in these areas. He is also the recipient of the IEEE Trans. on Industrial Informatics Best Paper Award in 2012, the European Union FP7 Marie Curie IRG Award in 2009, Turk Telekom Research Grant Awards in 2010 and 2012, and the San-Tez Project Awards supported by Alcatel-Lucent, and the Turkish Ministry of Science, Industry and Technology in 2010.